

(The following article has been accepted by Applied Physics Letters. After it is published, it will be found at <https://doi.org/10.1063/5.0102370>)

Rapid determination of single substitutional nitrogen N_s^0 concentration in diamond from UV-Vis spectroscopy

T. Luo,¹ L. Lindner,¹ R. Blinder,² M. Capelli,³ J. Langer,¹ V. Cimalla,¹ F. A. Hahl,¹ X. Vidal,¹ and J. Jeske¹

¹Fraunhofer Institute for Applied Solid State Physics IAF, 79108 Freiburg, Germany

²Ulm University, D-89081 Ulm, Germany

³School of Science, RMIT University, Melbourne VIC 3001, Australia

(*Electronic mail: jan.jeske@iaf.fraunhofer.de)

(Dated: 3 August 2022)

Single substitutional nitrogen atoms N_s^0 are the prerequisite to create nitrogen-vacancy (NV) centers in diamonds. They serve as the electron donors to create the desired NV^- center, provide charge stability against photo-ionisation, but also are the main source of decoherence. Therefore, precise and quick determination of N_s^0 concentration is a key advantage to a multitude of NV-related research in terms of material improvement as well as applications. Here we present a method to determine the N_s^0 concentration based on absorption spectroscopy in the UV-Visible range and fitting the 270 nm absorption band. UV-Visible spectroscopy has experimental simplicity and widespread availability that bear advantages over established methods. It allows a rapid determination of N_s^0 densities, even for large numbers of samples. Our method shows further advantages in determining low concentrations as well as the ability to measure locally, which is highly relevant for diamonds with largely varying N_s^0 concentrations in a single crystal. A cross-check with electron paramagnetic resonance (EPR) shows high reliability of our method and yields the absorption cross section of the 270 nm absorption band, $\sigma = 1.96 \pm 0.15 \text{ cm}^{-1} \cdot \text{ppm}^{-1}$ (in common logarithm) or $\sigma_e = 4.51 \pm 0.35 \text{ cm}^{-1} \cdot \text{ppm}^{-1}$ (in natural logarithm), which serves as a reference to determine N_s^0 concentrations, and makes our method applicable for others without the need for a known N_s^0 -reference sample and calibration. We provide a rapid, practical and replicable pathway that is independent of the machine used and can be widely implemented as a standard characterization method for the determination of N_s^0 concentrations.

Nitrogen is one of the main impurities in both natural and synthetic diamonds¹. Related defects, particularly the nitrogen-vacancy (NV) center, attract a broad interest for its special optical and spin properties^{2,3}. It has been extensively investigated for magnetometry⁴⁻⁸, bio-sensing^{9,10}, nuclear magnetic resonance (NMR)^{11,12} and scanning probe microscopy^{13,14}. To create NV centers, single substitutional nitrogen atoms, denoted as N_s^0 , P1 or C-centers, are the prerequisite. They are doped during the diamond growth or implanted on the diamond surface, followed by irradiation and annealing steps to create vacancies and allow NV centers to form. They play a role as the typical electron donor to charge the desired NV^- state¹⁵⁻¹⁸, and they are often present 10-100 times more than NV centers even in highly doped material. They determine the NV charge stability, and optimising the N_s^0 to NV^- conversion ratio is crucial for improving the NV center's performance and sensitivity¹⁹. Moreover, at parts-per-million (ppm) levels they can act as the main decoherence source of the NV center²⁰. Therefore, knowledge of the N_s^0 density gives significant advantages in the choice of material and performance in applications.

To measure the N_s^0 density in diamond, the established standard is electron paramagnetic resonance (EPR) spectroscopy²¹⁻²³. Field modulation is applied to record continuous wave EPR spectra, resulting in a spectrum that approximates the first derivative of the EPR line shape. Double integration of the acquired spectrum is taken to determine the EPR peak intensity and hence the N_s^0 concentration²⁴. Al-

though this method has been well established, it is often hard to access and labour-intensive, and its high requirement for the surface quality of diamond brings technical difficulties for the measurement. Moreover, the EPR method measures the spin number in the entire sample volume and averages different areas in the sample. For diamonds with less homogeneity, e.g. high-pressure, high-temperature (HPHT) diamonds that usually show sectors containing very different N_s^0 concentrations in a single crystal²⁵, the spatially resolved determination of the N_s^0 density can be of interest rather than the averaged value. In this regard, optical methods with experimental simplicity and widespread availability have significant advantages for many groups and companies working with NV centers, which makes the Fourier-transform infrared (FTIR) and UV-Visible (UV-Vis) spectroscopy favourable in some cases. Depending on the configuration of the spectrometer, both volume and spatially resolved measurements are possible by these optical methods.

The FTIR spectroscopy has been used to determine both N_s^0 (at 1130 cm^{-1} and 1344 cm^{-1})²⁶ and N_s^+ (at 1332 cm^{-1})²⁷ centers. For this method, a good spectral resolution is required, and different resolutions of the spectrometer have a significant effect on the concentration estimation²⁸. Moreover, for diamonds with low nitrogen densities less than a few tenths of ppm, the conventional FTIR spectroscopy often shows insufficient sensitivity in detecting these nitrogen-related centers²⁶. In comparison, the UV-Vis spectroscopy enables the detection of single nitrogen as low as 0.01 ppm ²⁹,

which is much below the detection limit of the conventional FTIR method. Furthermore, the UV-Vis spectroscopy with its experimental simplicity can be applied as a rapid method to characterize diamonds, especially for low nitrogen concentrations.

In the UV-Vis spectrum, the absorption band centered at 270 nm has been suggested to determine the N_s^0 concentration³⁰⁻³². Extracting the 270 nm band from the spectrum is thus a key step for this method. Different fitting methods have been introduced, but complex spectra and the simplistic nature of the literature methods leads to difficulties to determine the band reliably. Early on, Sumiya *et al.*³³ has suggested to subtract the spectrum at 270 nm with the ‘tail-line’, then calibrate this height with the EPR result. The ‘tail-line’ is a straight line fitted with the acquired spectrum at around 600-800 nm. This method provides a convenient approach which does not require complicated fitting. For diamonds without additional spectral components at the ‘tail’ region, it enables a quick and rough estimation of the N_s^0 concentration. When the diamond spectrum shows absorption bands that across the range (for example NV^- , NVN^- centers, or the nickel-related broad band centered at 710 nm, etc.), the method will be less accurate and even invalidated. Especially for chemical vapor deposition (CVD) diamonds, a perfect ‘tail’ without influence by other defects is unusual and difficult to achieve in nitrogen-doped growth.

A more advanced protocol has been introduced by Khan *et al.*^{34,35}, which avoids being dependent on the ‘tail’ region. This method relied on more complex fitting components: a ‘ramp’ in the form of λ^{-3} well fitting the overall decreasing trend of the absorption spectrum (which can be related to single vacancies¹⁹, or vacancy clusters^{36,37}); a combination of bands at 360 nm and 520 nm originate from vacancy clusters and NVH^0 centers respectively; and a ‘reference spectrum’ including the 270 nm band and its absorption continuum taken from a high-pressure, high-temperature (HPHT) type Ib diamond. The weight of the ‘reference spectrum’ then gives the strength of the 270 nm band and thus the N_s^0 concentration. This protocol improved the fitting accuracy significantly, it broadened applicable spectrum types as it was independent of absorption bands at 600-800 nm. Nevertheless, it is still limited by the HPHT reference spectrum that requires a detectable and clear 270 nm band. Besides, HPHT spectra have their own ‘ramp’ component and potentially other spectral features, using these as reference will not only isolate the 270nm peak but also fit the other components of the reference to the acquired spectrum. This creates a dependency on the utilised HPHT reference spectrum. Considering the fundamental difference in material properties between different synthesized diamonds, to avoid using a specific type of reference spectrum that contains the band of interest (270 nm) helps to reduce the fitting uncertainties and further improve the accuracy.

In this work, we present a fitting protocol to estimate N_s^0 concentrations reliably and precisely from the 270 nm band in the UV-Vis absorption spectrum. This protocol can be more generally adapted for complex spectra, especially for CVD diamonds. It also avoids the requirement for a reference spec-

trum with the band of interest and increases the fitting robustness. We furthermore calibrate this method with EPR measurements for a series of CVD diamonds with varying N_s^0 concentrations. From the calibration we find the linearity of the two methods and precision of our measurement. We deduce the absorption cross-section of the 270 nm band for N_s^0 , enabling the estimation of its concentrations without the requirement of a further reference sample with a known concentration.

We grew six (100) oriented CVD diamonds with varying nitrogen-doping levels for the method calibration. We pre-characterized their N_s^0 concentrations with an EPR spectrometer (Bruker ELEXSYS E580) at room temperature. The spectrometer was fitted with a Bruker super-high-Q probehead (ER4122 SHQE), and the microwave frequency was set to 9.84 GHz. N_s^0 concentrations were determined using the built-in spin-counting feature, from the acquisition software (xEPR). This measurement for N_s^0 concentration carries an error of $\sim 6\%$ (including the statistic error, the fitting error, and the accuracy of the EPR spectrometer). For details of the N_s^0 concentration see Table I.

To obtain the UV-Vis absorption spectra for the diamond, we measured the diamond transmission T in the range of 200-800 nm using an UV-Vis spectrometer (PerkinElmer Lambda 950) at room temperature, then we deduced the absorption coefficient A following the Lambert-Beer law: $A = -\log_{10}(T)/d$, where d is the sample thickness. Figure 1 shows a typical UV-Vis absorption spectrum of CVD diamonds, containing three absorption bands centered at respectively 270 nm, 360 nm and 520 nm. We fitted the spectrum with five components (Figure 1):

- Three Gaussian functions for the three typical bands in CVD diamonds $g_j(\lambda) = a_j \cdot \exp(-(\lambda - b_j)^2 / (2c_j^2))$, where a_j , b_j and c_j are the fitting parameters for each band $j=270, 360, 520$ (nm). Here 270 nm is the band of interest to extract the N_s^0 concentration, 360 nm corresponds to vacancy clusters and 520 nm to NVH^0 centers³⁵.

- A ‘ramp’ function $r(\lambda) = R \cdot \lambda^{-3}$ (same as in³⁴), where the factor R is the fitting parameter for this function.

- A spectrum ‘El-offset’, $e(\lambda)$, which is given by an electronic grade diamond (theoretically a ‘pure’ diamond without defect bands in the UV-Vis range). This reference spectrum is applied as an offset and baseline to the acquired spectrum, and it is also fitted with a coefficient d .

We fitted a sum of the five components to the original spectrum by a non-linear least squares fit:

$$Fit = g_{270}(\lambda) + g_{360}(\lambda) + g_{520}(\lambda) + r(\lambda) + d \cdot e(\lambda)$$

Different from previous works, here the key component, the 270 nm feature, is extracted as a Gaussian band. For this band (i.e. $g_{270}(\lambda)$ function), a lower- and upper-boundary of the fitting parameter have been introduced for the band-center b_{270} (268-272 nm) and the Gaussian RMS width c_{270} (13-27 nm), in order guide the algorithm to optimize the parameters in a small range. The boundaries were selected based on free fitting results of a large amount of samples, they also help to examine whether the fitting outcome exhibits reasonable values: if a final parameter is one of the boundary values, this indicates a unreliable fitting performance, i.e. the boundary

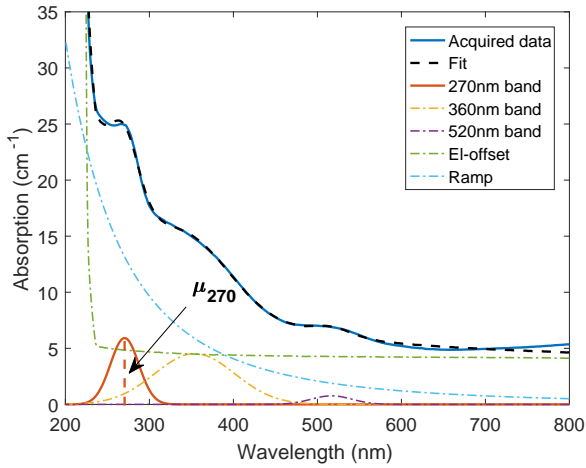


FIG. 1. Fitting for the UV-Vis absorption spectrum including three Gaussian bands at 270 nm, 360 nm and 520 nm, a ‘ramp’ function and an electronic-grade diamond spectrum as the offset. The fitting determines weighting factors to the components. The 270 nm band (red solid curve) can be taken as a direct indication of the concentration of N_s^0 .

has ‘forced’ the algorithm to stop while no optimization has been found in the expected range. On the contrary, if the final parameter exhibits a free value in the given range, the fitting was optimized correctly. For all our fits this condition was met.

With extracting the 270 nm band, we then compare its height, μ_{270} (in cm^{-1}), with the EPR measurements to investigate if the fitting result scales linearly to the EPR and thus can be validated. In this method, no reference sample with an ideal 270 nm band is required, the only reference spectrum in this method is the ‘El-offset’ component measured from the electronic grade diamond, which is an undoped diamond and thus avoids the variation which occurs in doped reference spectra. One can easily obtain this spectrum repeatedly from any ‘pure’ diamond, or simply use a literature spectrum as the offset for well-calibrated spectrometers.³⁸ This reduces the difficulty for implementing the fitting, and greatly avoids introducing undesired spectral components that vary from diamond to diamond. The ‘El-offset’ keeps the diamond intrinsic spectral feature (with an absorption edge at around 225-235 nm, then being ‘flat’ in the visible range up to 800 nm), instead of using a straight line as the offset. Importantly, considering that the 270 nm band is located very close to the absorption edge (~ 225 -235 nm), an additional parameter describing the sharp drop in this regime is necessary to supplement the ‘ramp’ function. In this sense, introducing the ‘El-offset’ can considerably improve the fitting performance.

For a spectrum with a weak or undetectable 520 nm band, i.e. for samples without NVH^0 centers potentially, the fitting method can be also adapted to four components. This can help to improve the fitting accuracy for some samples, as the fitting parameters for $g_{520}(\lambda)$ should be nearly zero in this sense, subtracting this band in the fitting function reduces unnecessary fitting parameters.

Figure 2 shows the fitting result for the six samples, they all show a good match between the fitting result and original spectrum. Mismatches appear at high wavelength (>650 nm), which is due to higher spectral features that are not included in the fitting. A possible candidate for these CVD diamonds can be H_2 centers (NV^-) with a zero-phonon line at 986 nm and a broad phonon side band centered at around 800 nm. For samples with strong features in this higher-wavelength regime (i.e. Cas-48, Cas-50 and Cas-68), a cut-off at 650 nm for the acquired data (i.e. fit for 200-650 nm) can improve the fitting performance. The good fitting result at lower wavelength shows that our method is independent of higher spectral features. The spectral variation around 650-800 nm illustrates the problem with defining a ‘tail’ as a baseline reference for the 270 nm peak³³.

As the next step, we compare the height of the extracted 270 nm Gaussian peak, μ_{270} , to the EPR result (Fig. 3). The good agreement of the two methods shown by the close-to-linear arrangement of the data points, proves the reliability of our fitting method. The 270 nm band has been assigned only to N_s^0 and has been used in several papers to determine only the N_s^0 concentration^{33-35,39}. We note however that an earlier research has suggested that the 270 nm band can be influenced by both N_s^0 and N_s^+ , especially for diamonds with low nitrogen concentrations⁴⁰, which has never been fully ruled out. Although our results can also not fully eliminate the possibility of a contribution of N_s^+ , the good linear fit of the EPR and UV-Vis results indicates that N_s^+ has minor influence if any. The discrepancies between the two methods in some previous works might have arisen from an inadequate fitting method for the spectrum. For more details of the band height and the EPR result see Table I.

From the slope in Figure 3, one can deduce the absorption cross-section σ of N_s^0 at 270 nm, with the relation:

$$\mu_{270} = \sigma \cdot [N_s^0] \quad (1)$$

where $[N_s^0]$ is the N_s^0 concentration in ppm, μ_{270} is the absorption coefficient of the extracted 270 nm band height (as described above). The theoretical derivation of the absorption cross-section is discussed in supplementary material. For common logarithm (i.e. decadic absorption coefficients), the absorption cross-section $\sigma = 1.96 \pm 0.15 \text{ cm}^{-1} \cdot \text{ppm}^{-1}$, the error is given by 95% confidence interval of the fitting parameter for the linear fit to the two methods. σ can be also given in cm^2 , i.e. $\sigma = (1.11 \pm 0.09) \times 10^{-17} \text{ cm}^2$, which is converted by multiplying a factor $10^6 m_C / \rho_{dia}$, where $m_C = 1.99 \times 10^{-23} \text{ g}$ is the atomic mass for ^{12}C and $\rho_{dia} = 3.51 \text{ g/cm}^3$ is the diamond density.

For the absorption coefficient calculated by natural logarithm, an absorption cross-section $\sigma_e = 4.51 \pm 0.35 \text{ cm}^{-1} \cdot \text{ppm}^{-1}$ should be applied instead. In previous research, we have found a single reference of the absorption cross-section at 270 nm²⁶, which has been stated as $1/\sigma = 0.6 \pm 0.1 \text{ ppm/cm}^{-1}$ (i.e. $\sigma = 1.67 \pm 0.28 \text{ cm}^{-1} \cdot \text{ppm}^{-1}$). However, the method of its determination, specifically how the spectrum has been separated was not stated. We thus assume our measurement is more precise, the values of these two completely independent

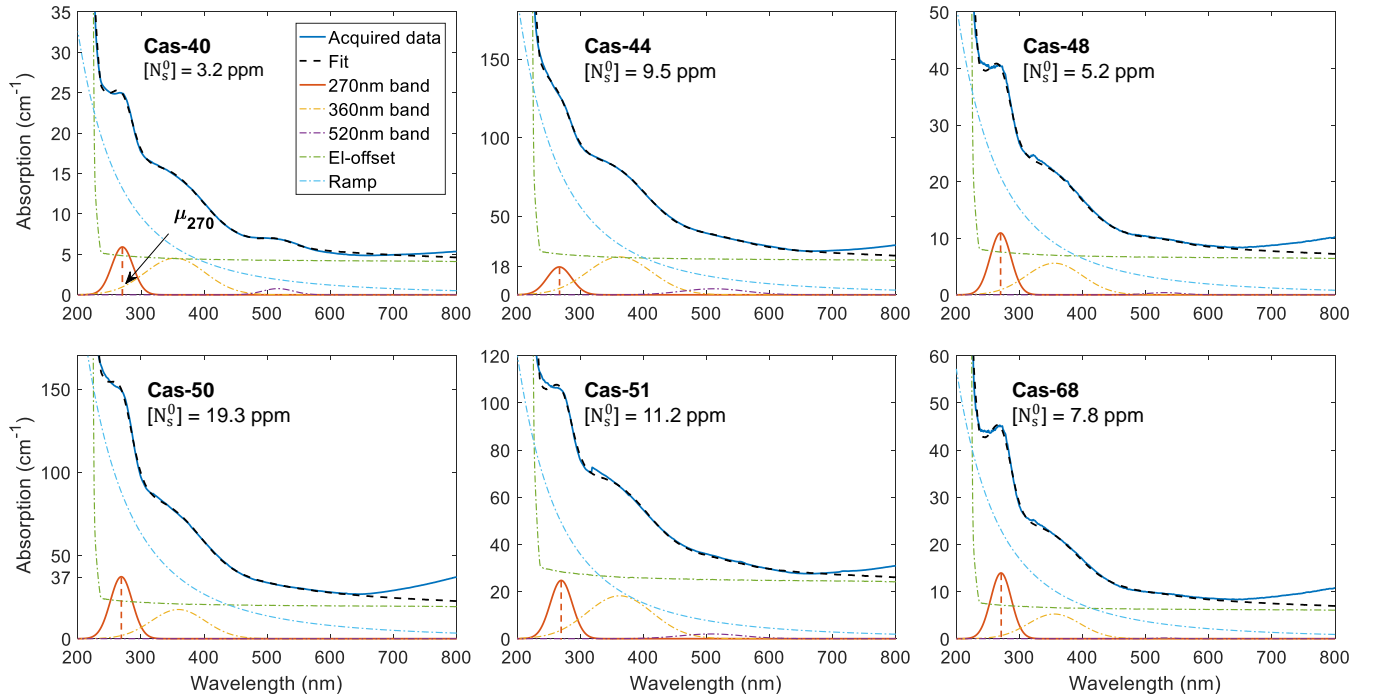


FIG. 2. Fitting result for all six samples. Details of the N_s^0 concentration and the peak height of 270 nm see Table I.

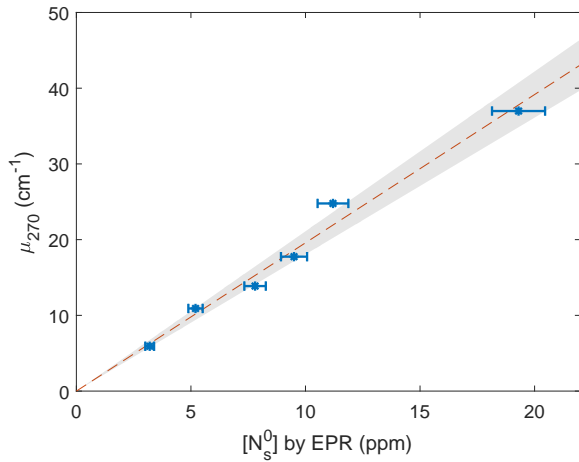


FIG. 3. The UV-Vis result by our fitting method is well aligned to the EPR result with a linear correlation. The linear fit shows a slope of $1.96 \pm 0.15 \text{ cm}^{-1} \cdot \text{ppm}^{-1}$ for μ_{270} given by decadic absorption coefficients. The error of the slope is given by 95% confidence interval of the fitting parameter (gray area in the plot).

measurements are remarkably close.

From our protocol, one can estimate $[N_s^0]$ directly from their UV-Vis spectra, without calibrating by other methods. This can be achieved for any samples with both sides polished in the following way: Firstly measure the UV-Vis transmission in percentage then convert it into the absorption spectrum in cm^{-1} ; secondly separate the spectrum to extract the 270 nm band and obtain μ_{270} according to the method de-

scribed above; finally calculate the N_s^0 concentration using Equation (1) with the absorption cross-section σ or σ_e (depending on the logarithm type when deducing the absorption from transmission). The method is setup-independent and applicable for UV-Vis spectra taken by any machine, whether by volume measurements or spatially resolved measurements. No further EPR/FTIR measurements are required, as Equation (1) gives the absolute value of the N_s^0 concentration and our value for sigma can be used.

TABLE I. Details of the samples and results. The N_s^0 concentration $[N_s^0]$ was measured by EPR, which brings an error of around $\pm 6\%$. The fitting for μ_{270} has an error of $\lesssim 1\%$.

Sample	$[N_s^0]$ (ppm)	μ_{270} (cm^{-1})
Cas-40	3.2	5.9
Cas-44	9.5	17.7
Cas-48	5.2	10.9
Cas-50	19.3	37.2
Cas-51	11.2	24.7
Cas-68	7.8	13.9

We developed a fitting method for determining N_s^0 concentration via UV-Vis absorption spectrum, which is more widely accessible and easily implementable than EPR measurements. We showed that the fitting of the identified bands is a reliable way to extract the 270 nm band from the background, as seen by the good match between measurement and fit, and confirmed by the linear relationship between EPR result and our method. The good agreement with EPR furthermore confirms the assumption that the 270 nm band indeed is mainly caused

by N_s^0 . Our fitting method performs well for diamond spectra without complex components overlapping with the the fitting components. In other words, it can be widely applied to different diamond types apart from as-grown CVD diamonds.

Furthermore, we deduced the absorption cross-section $\sigma = 1.96 \pm 0.15 \text{ cm}^{-1} \cdot \text{ppm}^{-1}$ (for common logarithm) and $\sigma_e = 4.51 \pm 0.35 \text{ cm}^{-1} \cdot \text{ppm}^{-1}$ (for natural logarithm), which can serve to rapidly determine N_s^0 densities from UV-Vis measurements without the need to calibrate a setup via EPR. This also enables the determination of N_s^0 concentrations in a lower end that is hardly detectable by EPR or FTIR methods. The detectable range of N_s^0 concentration is limited by the sensitivity of the UV-Vis spectrometer. Based on our spectrometer, we estimated a detectable range for typical 300 μm diamond plates from 0.01 ppm to 30-50 ppm (details are discussed in supplementary material). For thinner/thicker samples, the determination of higher/lower N_s^0 concentrations are also possible. The range can be expanded by orders of magnitude with more sensitive spectrometers. The fitting protocol combined with the calibrated absorption cross-section provide a rapid, easy and replicable pathway for the standardized determination of N_s^0 concentrations for future research.

SUPPLEMENTARY MATERIAL

See supplementary material for the discussion of the detectable range of N_s^0 concentration and the theoretical derivation of the absorption cross-section.

We thank Brant Gibson, Andrew Greentree, Peter Knittel, Christian Giese, Christoph Schreyvogel and Oliver Ambacher for valuable discussions. We thank Fedor Jelezko for valuable discussions and supports of the EPR theory. We thank Michael Ardner, Christine Lell and Michaela Fritz for preparing diamond plates, Dorothee Luick for the technical support of UV-Vis measurements. T.L and J.J acknowledge the funding by the German federal ministry for education and research Bundesministerium für Bildung und Forschung (BMBF) under Grant No. 13XP5063. M.C. acknowledges funding from the Asian Office of Aerospace Research and Development (AOARD, funding FA2386-18-1-4056).

The data that support the findings of this study are available from the corresponding author upon reasonable request.

- ¹M. N. Ashfold, J. P. Goss, B. L. Green, P. W. May, M. E. Newton, and C. V. Peaker, "Nitrogen in diamond," *Chemical reviews* **120**, 5745–5794 (2020).
- ²I. Aharonovich, A. D. Greentree, and S. Praver, "Diamond photonics," *Nature Photonics* **5**, 397–405 (2011).
- ³M. W. Doherty, N. B. Manson, P. Delaney, F. Jelezko, J. Wrachtrup, and L. C. Hollenberg, "The nitrogen-vacancy colour centre in diamond," *Physics Reports* **528**, 1–45 (2013).
- ⁴C. Degen, "Scanning magnetic field microscope with a diamond single-spin sensor," *Applied Physics Letters* **92**, 243111 (2008).
- ⁵V. M. Acosta, E. Bauch, M. P. Ledbetter, C. Santori, K.-M. Fu, P. E. Barclay, R. G. Beausoleil, H. Linget, J. F. Roch, F. Treussart, *et al.*, "Diamonds with a high density of nitrogen-vacancy centers for magnetometry applications," *Physical Review B* **80**, 115202 (2009).
- ⁶L. Rondin, J.-P. Tetienne, T. Hingant, J.-F. Roch, P. Maletinsky, and V. Jacques, "Magnetometry with nitrogen-vacancy defects in diamond," *Reports on progress in physics* **77**, 056503 (2014).
- ⁷J. Jeske, J. H. Cole, and A. D. Greentree, "Laser threshold magnetometry," *New Journal of Physics* **18**, 013015 (2016).
- ⁸F. A. Hahl, L. Lindner, X. Vidal, T. Luo, T. Ohshima, S. Onoda, S. Ishii, A. M. Zaitsev, M. Capelli, B. C. Gibson, *et al.*, "Magnetic-field-dependent stimulated emission from nitrogen-vacancy centers in diamond," *Science Advances* **8**, eabn7192 (2021).
- ⁹R. Schirhagl, K. Chang, M. Loretz, and C. L. Degen, "Nitrogen-vacancy centers in diamond: nanoscale sensors for physics and biology," *Annual review of physical chemistry* **65**, 83–105 (2014).
- ¹⁰Y. Wu, F. Jelezko, M. B. Plenio, and T. Weil, "Diamond quantum devices in biology," *Angewandte Chemie International Edition* **55**, 6586–6598 (2016).
- ¹¹D. R. Glenn, D. B. Bucher, J. Lee, M. D. Lukin, H. Park, and R. L. Walsworth, "High-resolution magnetic resonance spectroscopy using a solid-state spin sensor," *Nature* **555**, 351–354 (2018).
- ¹²D. B. Bucher, D. P. Aude Craik, M. P. Backlund, M. J. Turner, O. Ben Dor, D. R. Glenn, and R. L. Walsworth, "Quantum diamond spectrometer for nanoscale nmr and esr spectroscopy," *Nature Protocols* **14**, 2707–2747 (2019).
- ¹³A. W. Schell, G. Kewes, T. Schröder, J. Wolters, T. Aichele, and O. Benson, "A scanning probe-based pick-and-place procedure for assembly of integrated quantum optical hybrid devices," *Review of Scientific Instruments* **82**, 073709 (2011).
- ¹⁴T. X. Zhou, R. J. Stöhr, and A. Yacoby, "Scanning diamond nv center probes compatible with conventional afm technology," *Applied Physics Letters* **111**, 163106 (2017).
- ¹⁵A. T. Collins, "The fermi level in diamond," *Journal of Physics: Condensed Matter* **14**, 3743 (2002).
- ¹⁶K.-M. Fu, C. Santori, P. Barclay, and R. Beausoleil, "Conversion of neutral nitrogen-vacancy centers to negatively charged nitrogen-vacancy centers through selective oxidation," *Applied Physics Letters* **96**, 121907 (2010).
- ¹⁷A. Haque and S. Sumaiya, "An overview on the formation and processing of nitrogen-vacancy photonic centers in diamond by ion implantation," *Journal of Manufacturing and Materials Processing* **1**, 6 (2017).
- ¹⁸M. Hauf, B. Grotz, B. Naydenov, M. Dankerl, S. Pezzagna, J. Meijer, *et al.*, "Chemical control of the charge state of nitrogen-vacancy centers in diamond," *Physical Review B* **83**, 081304 (2011).
- ¹⁹T. Luo, L. Lindner, J. Langer, V. Cimalla, X. Vidal, F. Hahl, C. Schreyvogel, S. Onoda, S. Ishii, T. Ohshima, *et al.*, "Creation of nitrogen-vacancy centers in chemical vapor deposition diamond for sensing applications," *New Journal of Physics* **24**, 033030 (2022).
- ²⁰E. Bauch, S. Singh, J. Lee, C. A. Hart, J. M. Schloss, M. J. Turner, *et al.*, "Decoherence of ensembles of nitrogen-vacancy centers in diamond," *Physical Review B* **102**, 134210 (2020).
- ²¹W. Smith, P. Sorokin, I. Gelles, and G. Lasher, "Electron-spin resonance of nitrogen donors in diamond," *Physical Review* **115**, 1546 (1959).
- ²²J. Van Wyk, E. Reynhardt, G. High, and I. Kiflawi, "The dependences of esr line widths and spin-spin relaxation times of single nitrogen defects on the concentration of nitrogen defects in diamond," *Journal of Physics D: Applied Physics* **30**, 1790 (1997).
- ²³G. R. Eaton, S. S. Eaton, D. P. Barr, and R. T. Weber, *Quantitative Epr* (Springer Science & Business Media, 2010).
- ²⁴A. Tallaire, A. Collins, D. Charles, J. Achard, R. Sussmann, A. Gicquel, M. Newton, A. Edmonds, and R. Cruddace, "Characterisation of high-quality thick single-crystal diamond grown by cvd with a low nitrogen addition," *Diamond and related materials* **15**, 1700–1707 (2006).
- ²⁵M. Capelli, A. Heffernan, T. Ohshima, H. Abe, J. Jeske, A. Hope, *et al.*, "Increased nitrogen-vacancy centre creation yield in diamond through electron beam irradiation at high temperature," *Carbon* **143**, 714–719 (2019).
- ²⁶I. A. Dobrinets, V. G. Vins, and A. M. Zaitsev, *HPHT-treated diamonds* (Springer, 2016).
- ²⁷S. C. Lawson, D. Fisher, D. C. Hunt, and M. E. Newton, "On the existence of positively charged single-substitutional nitrogen in diamond," *Journal of Physics: Condensed Matter* **10**, 6171 (1998).
- ²⁸S. Liggins, *Identification of point defects in treated single crystal diamond*, Ph.D. thesis, University of Warwick (2010).
- ²⁹F. De Weerd and A. Collins, "Determination of the c defect concentration in hpht annealed type iaa diamonds from uv-vis absorption spectra," *Diamond and related materials* **17**, 171–173 (2008).
- ³⁰H. Dyer, F. Raal, L. Du Preez, and J. Loubser, "Optical absorption features associated with paramagnetic nitrogen in diamond," *Philosophical Magazine* **11**, 763–774 (1965).
- ³¹R. Chrenko, H. Strong, and R. Tuft, "Dispersed paramagnetic nitrogen

- content of large laboratory diamonds,” *Philosophical Magazine* **23**, 313–318 (1971).
- ³²J. Walker, “Optical absorption and luminescence in diamond,” *Reports on progress in physics* **42**, 1605 (1979).
- ³³H. Sumiya and S. Satoh, “High-pressure synthesis of high-purity diamond crystal,” *Diamond and Related Materials* **5**, 1359–1365 (1996).
- ³⁴R. U. A. Khan, P. M. Martineau, B. Cann, M. Newton, and D. Twitchen, “Charge transfer effects, thermo and photochromism in single crystal cvd synthetic diamond,” *Journal of Physics: Condensed Matter* **21**, 364214 (2009).
- ³⁵R. Khan, B. Cann, P. Martineau, J. Samartseva, J. Freeth, S. Sibley, C. Hartland, M. Newton, H. Dhillon, and D. Twitchen, “Colour-causing defects and their related optoelectronic transitions in single crystal cvd diamond,” *Journal of Physics: Condensed Matter* **25**, 275801 (2013).
- ³⁶J.-M. Mäki, F. Tuomisto, C. Kelly, D. Fisher, and P. Martineau, “Effects of thermal treatment on optically active vacancy defects in cvd diamonds,” *Physica B: Condensed Matter* **401**, 613–616 (2007).
- ³⁷R. Jones, “Dislocations, vacancies and the brown colour of cvd and natural diamond,” *Diamond and related materials* **18**, 820–826 (2009).
- ³⁸We can provide the spectrum data for the ‘El-offset’ and other technical assistance upon request.
- ³⁹A. M. Edmonds, C. A. Hart, M. J. Turner, P.-O. Colard, J. M. Schloss, K. S. Olsson, R. Trubko, M. L. Markham, A. Rathmill, B. Horne-Smith, *et al.*, “Characterisation of cvd diamond with high concentrations of nitrogen for magnetic-field sensing applications,” *Materials for Quantum Technology* **1**, 025001 (2021).
- ⁴⁰R. Jones, J. Goss, and P. Briddon, “Acceptor level of nitrogen in diamond and the 270-nm absorption band,” *Physical Review B* **80**, 033205 (2009).